Myocardial ^{11}C-Diacylglycerol Accumulation and Left Ventricular Remodeling in Patients After Myocardial Infarction

Hiroki Otani, MD, PhD[1]; Yutaka Kagaya, MD, PhD[1]; Yoshio Imahori, MD, PhD[2]; Satoshi Yasuda, MD, PhD[3]; Ryo Fujii, PhD[4]; Masanobu Chida, MD, PhD[1]; Shigeto Namiuchi, MD, PhD[1]; Morihiko Takeda, MD, PhD[1]; Masahito Sakuma, MD, PhD[1]; Jun Watanabe, MD, PhD[1]; Tatsuo Ido, PhD[5]; Hiroshi Nonogi, MD, PhD[3]; and Kunio Shirato, MD, PhD[1]

[1]Department of Cardiovascular Medicine, Tohoku University Graduate School of Medicine, Sendai, Japan; [2]Department of Neurosurgery, Kyoto Prefectural University of Medicine, Kyoto, Japan; [3]Division of Cardiology, National Cardiovascular Center, Osaka, Japan; [4]Nishijin Hospital, Kyoto, Japan; and [5]Cyclotron and Radioisotope Center, Tohoku University, Sendai, Japan

Left ventricular (LV) remodeling after myocardial infarction (MI) is a maladaptive process that increases the risk of heart failure and death. The myocardial phosphoinositide cycle, which is located downstream from several neurohumoral factors, plays a crucial role in LV remodeling. Our animal studies demonstrated that 1-[1-^{11}C]butyryl-2-palmitoyl-rac-glycerol (^{11}C-DAG) can be used to visualize regions with an activated phosphoinositide cycle. Therefore, we examined whether myocardial ^{11}C-DAG accumulation assessed by PET is relevant to LV enlargement and systolic dysfunction in post-MI patients. **Methods:** We performed PET with ^{11}C-DAG in 13 post-anteroseptal MI patients and 4 healthy volunteers. We placed regions of interest on the noninfarcted myocardium and calculated the myocardium-to-left atrial (LA) chamber ratio of ^{11}C-DAG accumulation. **Results:** The myocardium-to-LA chamber ratio of ^{11}C-DAG was significantly higher in the post-MI patients (mean $\pm$ SD, 1.73 $\pm$ 0.35) compared with that of the healthy volunteers (mean $\pm$ SD, 1.25 $\pm$ 0.13; $P < 0.05$). In the post-MI patients, the myocardium-to-LA chamber ratio of ^{11}C-DAG was significantly correlated with the LV end-diastolic volume index ($r = 0.79$, $P < 0.01$) and the plasma concentration of brain natriuretic peptide ($r = 0.85$, $P < 0.001$) and negatively correlated with the LV ejection fraction ($r = -0.69$, $P < 0.01$). **Conclusion:** These findings suggest that the myocardial ^{11}C-DAG accumulation assessed by PET is relevant to LV enlargement, LV systolic dysfunction, and humoral activation in post-MI patients. This new imaging strategy based on intracellular signaling may contribute to the assessment and treatment of post-MI patients.

Key Words: myocardial infarction; ventricular remodeling; signal transduction

J Nucl Med 2005; 46:553–559

Left ventricular (LV) remodeling, the expansion of the infarct zone and characteristic changes in the noninfarcted myocardium (e.g., cardiomyocyte hypertrophy, interstitial fibrosis, and impaired contraction and relaxation, etc.), is a maladaptive process that causes deterioration of the LV function and increases the risk of congestive heart failure as well as cardiovascular death after myocardial infarction (MI) (1). The Survival and Ventricular Enlargement (SAVE) trial and other randomized clinical trials have shown that angiotensin-converting enzyme inhibitors prevent LV remodeling and the worsening of heart failure and decrease cardiovascular death in post-MI patients (2–5). The results of these trials strongly suggest that the rennin–angiotensin system plays a pivotal role in the development of LV remodeling and the resultant worsening of heart failure in post-MI patients.

The phosphoinositide cycle is an intracellular signal transduction system located at the downstream pathways of $G_{q\alpha}$ protein and phospholipase $C_{\beta 1}$, which couples with angiotensin II, endothelin-1, and α_1-adrenergic receptors (6), and plays a key role in LV remodeling after MI. One of the important second messengers of the phosphoinositide cycle is diacylglycerol. Diacylglycerol activates protein kinase C, which has been shown to play an important isozyme-specific role in the development of cardiac hypertrophy and failure (7–10). Therefore, noninvasive assessment of the myocardial phosphoinositide cycle in post-MI patients might provide a useful tool to assess the development of LV remodeling and might contribute to optimizing treatments that ameliorate post-MI LV remodeling and heart failure.

We previously reported that intravenously administered 1-[1-^{11}C]butyryl-2-palmitoyl-rac-glycerol (^{11}C-DAG), a ^{11}C-labeled diacylglycerol, was metabolized to the intermediates of the phosphoinositide cycle in the rat brain and that cholinergic stimulation prompted the accumulation of [11]C-

DAG (*11*). We also reported that intravenously administered ^{11}C-DAG was also predominantly metabolized to the intermediates of the phosphoinositide cycle in the rat infarcted heart and enabled successful visualization of the myocardial region with the activated phosphoinositide cycle (*12*). Furthermore, we demonstrated that the angiotensin-converting enzyme inhibitor captopril suppressed the accelerated myocardial ^{11}C-DAG accumulation in the infarcted rat heart (*13*). The results of these previous studies show that accelerated myocardial accumulation of ^{11}C-DAG reflects the activated phosphoinositide cycle. It is unclear whether the myocardial phosphoinositide cycle also plays a key role in post-MI LV remodeling in humans. In the present study, we investigated the hypothesis that myocardial accumulation of ^{11}C-DAG assessed by PET is relevant to LV enlargement and LV systolic dysfunction in post-MI patients.

MATERIALS AND METHODS

Patients

We studied 13 patients (7 men; mean age $\pm$ SD, 68 $\pm$ 7 y) with LV dysfunction due to previous anteroseptal Q-wave MI 4–53 mo after MI. The clinical characteristics of the patients are shown in Table 1. The diagnosis of MI was based on a typical medical history, electrocardiographic changes, and biochemical detection of cardiac enzyme release, although the maximum creatine kinase level was uncertain in 3 patients. Eight patients underwent primary percutaneous coronary intervention for the left anterior descending coronary artery, resulting in thrombolysis in myocardial infarction (TIMI) grade III of the coronary flow. In one patient, rescue percutaneous coronary intervention followed unsuccessful coronary thrombolysis. In 4 patients, percutaneous coronary intervention for the residual narrowing or occlusion of the left anterior descending coronary artery was performed in the chronic phase because spontaneous recanalization had occurred in the acute phase or they had not been considered as candidates for the

TABLE 1
Clinical Characteristics and Myocardium/LA Chamber Ratio of ^{11}C-DAG of Post-MI Patients and Healthy Volunteers

Subject no.	Age (y)	Sex	Period after MI (mo)	CK maximum (IU/L)	BNP (pg/mL)	LVEF (%)	LVEDVI (mL/m^2)	Medication (per day)	^{11}C-DAG counts (cps/MBq/kg) In LV myocardium	In LA chamber	Myocardium/LA chamber ratio of ^{11}C-DAG
Post-MI patients											
1	66	F	31	6,794	128	27	81	Lisinopril (5 mg), metoprolol (120 mg)	40.5	23.9	1.69
2	69	M	7	9,267	210	19	90	Imidapril (5 mg), carvedilol (10 mg)	32.9	16.3	2.01
3	79	M	4	5,330	130	33	56	Lisinopril (10 mg), bisoprolol (2.5 mg)	19.7	13.5	1.46
4	62	F	53	NA	599	21	178	Imidapril (5 mg)	52.3	20.3	2.58
5	72	M	42	8,122	127	29	82	Enalapril (2.5 mg)	31.3	17.0	1.84
6	58	F	7	NA	46	37	61	None	26.6	19.1	1.39
7	71	F	11	4,191	50	37	60	Temocapril (4 mg)	26.4	17.0	1.56
8	66	M	35	11,789	149	37	123	None	36.2	23.7	1.52
9	58	F	12	12,000	221	19	143	Cadesartan (4 mg), carvedilol (15 mg)	63.5	30.0	2.12
10	76	M	15	1,312	84	46	79	Enalapril (5 mg), metoprolol (80 mg)	56.3	42.1	1.34
11	74	M	7	1,854	99	48	58	Enalapril (2.5 mg), metoprolol (60 mg)	58.9	35.5	1.66
12	62	F	23	3,223	11	51	74	None	26.5	17.4	1.53
13	72	M	8	NA	45	43	81	Temocapril (2 mg), metoprolol (60 mg)	46.7	25.6	1.82
Mean	68		20	6,388	146	34	90		39.8	23.2	1.73
SD	7		16	3,865	150	11	37		14.3	8.3	0.35
Healthy volunteers											
14	24	M		NA	NA	NA	NA	None	24.1	18.8	1.28
15	24	M		NA	NA	NA	NA	None	23.3	21.7	1.08
16	34	M		NA	NA	NA	NA	None	27.3	19.8	1.38
17	23	M		NA	NA	NA	NA	None	23.9	18.9	1.26
Mean	26								24.7	19.8	1.25
SD	5								1.8	1.3	0.13

LA = left atrium; CK = creatine kinase; BNP = brain natriuretic peptide; LVEF = LV ejection fraction; LVEDVI = LV end-diastolic volume index; NA = not available.

reperfusion therapy in the acute phase. No patients had a significant coronary artery stenosis in the right or left circumflex coronary arteries. All post-MI patients were New York Heart Association functional class 1 or 2, and none had an episode of worsening of heart failure requiring hospital admission within 3 mo of the PET study. Nine post-MI patients had been treated with angiotensin-converting enzyme inhibitors and one post-MI patient had been treated with angiotensin II type 1 receptor antagonist. Seven post-MI patients had been treated with β-blockers. Plasma brain natriuretic peptide (BNP) concentrations were assessed with a highly sensitive radioimmunoassay kit (Shionoria BNP; Shionogi) 17 ± 18 mo (mean $\pm$ SD) after the onset of acute MI when they were in a very stable condition. We also studied 4 healthy volunteers (mean age $\pm$ SD, 26 ± 5 y). None of the healthy volunteers had abnormal echocardiographic findings. The purpose and nature of the present study were approved by the ethics committees of our institutes. Written informed consent was obtained from every subject before the study.

Echocardiography and Cardiac Catheterization

We performed echocardiography in all patients and healthy volunteers. Examinations were performed while the subjects were in the left lateral recumbent position. Standard echocardiographic views of the LV were obtained, and end-diastolic and end-systolic dimensions and wall thickness of the interventricular septum and the LV posterior wall were determined. LV dimensions were measured according to the recommendations of the American Society of Echocardiography (14).

We performed cardiac catheterization in all post-MI patients within 5.2 ± 7.0 mo (mean $\pm$ SD) after the onset of MI when the patients were in a very stable condition. The biplane LV angiograms were filmed using right and left anterior oblique views, and the LV end-diastolic and end-systolic volumes were estimated using the area–length method (15).

Synthesis of ¹¹C-DAG

¹¹C-DAG was synthesized as previously described in detail (11,16). Briefly, ¹¹C-ethylketene, which was synthesized using a cyclotron, was trapped in a pyridine solution containing 1 μmol/L 2-palmitoylglycerol. The acylation reaction was performed using ¹¹C-ethylketene under no-carrier-added conditions. ¹¹C-DAG had a high specific activity of 186 GBq/μmol at the end of synthesis. Radiochemical purity of ¹¹C-DAG was 98% at the time of injection. Human application and quality control of ¹¹C-DAG followed the guidelines established by the Committee of PET in Nishijin Hospital (Kyoto, Japan).

PET

We performed PET in post-MI patients (20 ± 16 mo [mean $\pm$ SD] after the onset of acute MI) and healthy volunteers using a Headtome IV (Shimadzu; in-plane full width at half maximum [FWHM], 4.5 mm; axial FWHM, 11.0 mm; axial field of view, 9 cm; number of planes, 21). After transmission scanning to correct attenuation, we first performed PET after the inhalation of ¹⁵O-carbon monoxide to visualize the left atrial (LA) and LV chambers. After the ¹⁵O radioactivity in the blood pool returned to the baseline level, we injected 1,110 MBq of ¹¹C-DAG intravenously. Since the ¹¹C radioactivity in the blood pool became sufficiently low to allow appropriate contrast between the blood pool and noninfarcted myocardium approximately 20 min after the ¹¹C-DAG injection, we collected static data from 15 to 27 min after the injection. We generated the short axial slices of the heart (matrix size, 128×128; pixel size, 2 mm; slice thickness, 6 mm) and placed 12–18 circular regions of interest (ROIs) (diameter, 11.0 mm) on the noninfarcted myocardium (the inferior and lateral wall of the LV) using 3 basal short axial slices in each subject. We also placed 4–6 circular ROIs (diameter, 11.0 mm) in the LA chamber using 2 short axial slices of the LA. We did not correct the partial-volume effect on the recovery of counts in the present study. Then, we calculated the myocardium-to-LA chamber ratio of ¹¹C-DAG accumulation by dividing the average counts of ¹¹C-DAG in the inferior and lateral wall by the counts of ¹¹C-DAG in the LA chamber.

Statistical Analysis

All values are expressed as mean $\pm$ SD. Statistical analysis of differences between groups was done by the unpaired Student t test. A correlation between the 2 parameters was determined by simple linear regression analysis. Statistical significance was accepted at a level of $P < 0.05$.

RESULTS

The clinical characteristics of the post-MI patients and the healthy volunteers are shown in Table 1. Figure 1 shows the short axial slices of PET with ¹¹C-DAG of a healthy volunteer and 2 post-MI patients (patients 6 and 4). The myocardium-to-LA chamber ratio of ¹¹C-DAG was significantly increased in the post-MI patients (1.73 ± 0.35) compared with that of the healthy volunteers (1.25 ± 0.13, $P < 0.05$; Fig. 2). In the post-MI patients, the myocardium-to-LA chamber ratio of ¹¹C-DAG significantly correlated with the LV end-diastolic volume index ($r = 0.79$, $P < 0.01$; Fig. 3A) and the plasma concentration of BNP ($r = 0.85$, $P < 0.001$; Fig. 3C) and negatively correlated with the LV ejection fraction ($r = -0.69$, $P < 0.01$; Fig. 3B). Although we had one patient with a highly increased BNP level, the correlation between the myocardium-to-LA chamber ratio of ¹¹C-DAG and the BNP level was still significant after excluding this patient ($r = 0.64$, $P < 0.05$).

Possibly, the difference in the wall thickness among the subjects might have affected the results demonstrated in Figures 2 and 3 through the partial-volume effect. However, the wall thickness of post-MI patients determined by echocardiography was not significantly increased compared with that of the healthy volunteers in both the interventricular septum (8.6 ± 1.5 vs. 7.7 ± 0.5 mm, respectively) and the LV posterolateral wall (9.3 ± 1.3 vs. 8.0 ± 0.8 mm, respectively). Furthermore, the myocardium-to-LA chamber ratio of ¹¹C-DAG did not correlate with the myocardial wall thickness of the LV posterior wall ($r = 0.11$, $P = 0.73$) that were determined by echocardiography.

DISCUSSION

In the present study, we demonstrated that the myocardial accumulation of ¹¹C-DAG in the remote viable myocardium of post-MI patients was significantly increased compared with that of the healthy volunteers. Furthermore, the accumulation of ¹¹C-DAG in the post-MI patients significantly
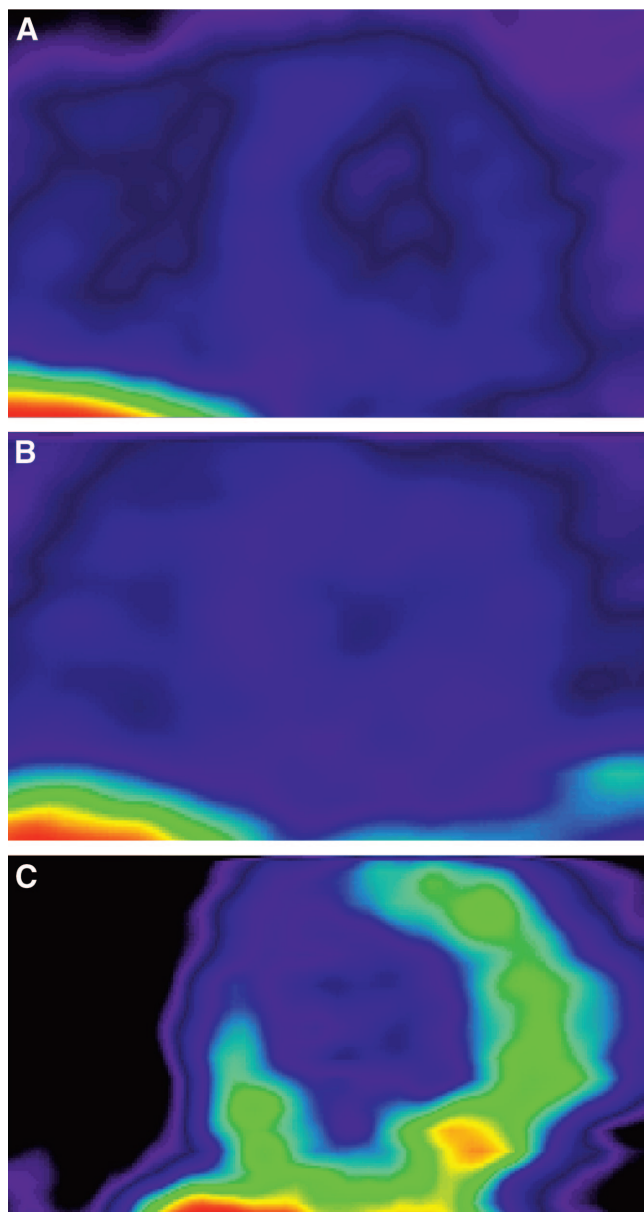
FIGURE 1. Representative short axial slices of PET with ^{11}C-DAG in healthy volunteer (A) and 2 post-MI patients (B and C). In healthy volunteer, myocardial accumulation of ^{11}C-DAG was mild and myocardium-to-LA chamber ratio of ^{11}C-DAG was 1.28 (A). In post-MI patient 6, myocardial accumulation of ^{11}C-DAG was also mild and myocardium-to-LA chamber ratio of ^{11}C-DAG was 1.39 (B). In patient 4, a remarkable accumulation of ^{11}C-DAG was observed in remote viable myocardium (inferior septum and inferolateral wall). Myocardium-to-LA chamber ratio of ^{11}C-DAG was 2.58 (C).

correlated with the LV enlargement, LV systolic dysfunction, and plasma BNP levels.

### Mechanism of ^{11}C-DAG Accumulation

In our previous studies (11,17,18), we reported that intravenously administered ^{11}C-DAG was metabolized to the intermediates of the phosphoinositide cycle—that is, phosphatidic acids, phosphatidylinositols, and phosphatidylino-

sitol phosphates in the rat brain—and that cholinergic stimulation promoted the accumulation of ^{11}C radioactivity. These results suggest that ^{11}C-DAG accumulation in the rat brain reflects the phosphoinositide metabolic process, which is stimulated by cholinergic neurotransmission (11). Furthermore, in our recent study (12), we administered ^{11}C-DAG intravenously to rats 7 d after MI to investigate the metabolic fate of ^{11}C-DAG in myocardium. In that study, thin-layer chromatography of ^{11}C-DAG metabolites obtained from both infracted and noninfarcted myocardium revealed that intermediates of the phosphoinositide cycle were the predominant metabolites in both infarcted and noninfarcted myocardium (12). In our more recent study using the same acute MI model in rats, the accelerated myocardial ^{11}C-DAG accumulation 3 wk after the onset of MI was significantly suppressed by a 3-wk captopril treatment that was initiated immediately after the onset of MI (13). These results from our previous animal studies suggest that intravenously administered ^{11}C-DAG was predominantly metabolized to intermediates of the phosphoinositide cycle and that myocardial accumulation of ^{11}C-DAG depends on the activity of the phosphoinositide cycle, which is located downstream of angiotensin II, endothelin-1, and α_1-adrenergic receptors.

Myocardial ^{11}C-DAG Accumulation and LV Remodeling

As shown in Figure 2, the myocardial accumulation of ^{11}C-DAG in the post-MI patients was relatively scattered. As shown in Table 1, LV end-diastolic volume was not enlarged and LV ejection fraction was well preserved in some post-MI patients, presumably due to early coronary reperfusion performed in these patients. In fact, the average myocardium-to-LA chamber ratio of ^{11}C-DAG of 6 post-MI patients whose LV end-diastolic volume index was <80 mL/m² was 1.45 ± 0.13. This value was not significantly different from those of the healthy volunteers. We then investigated the relationship between myocardial ^{11}C-DAG
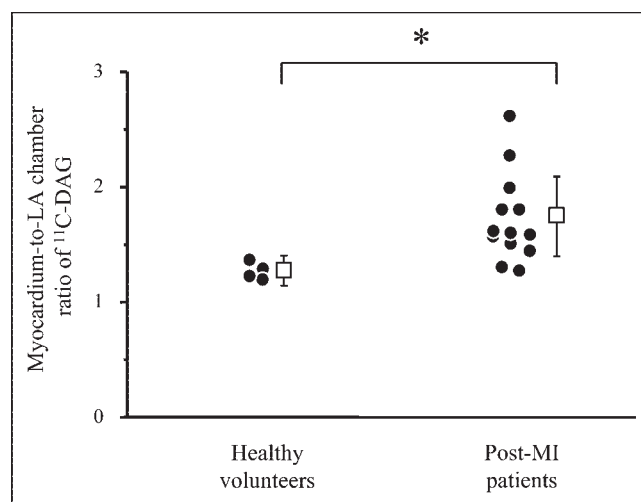
FIGURE 2. Myocardium-to-LA chamber ratio of ^{11}C-DAG in healthy volunteers and post-MI patients. *$P < 0.05$.
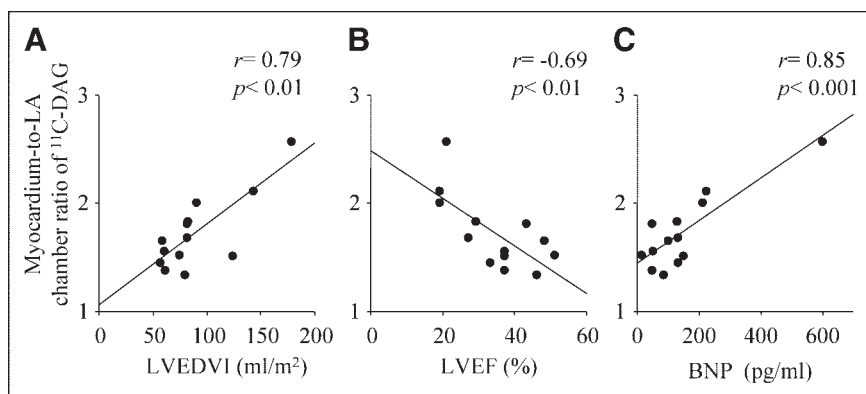
FIGURE 3. Correlations between myocardium-to-LA chamber ratio of ^{11}C-DAG and LVEDVI (A), LVEF (B), and plasma concentration of BNP (C). LVEDVI = left ventricular end-diastolic volume index; LVEF = left ventricular ejection fraction.

accumulation and LV end-diastolic volume, LV ejection fraction, and plasma BNP level in post-MI patients and found that the myocardial accumulation of ^{11}C-DAG correlated with these parameters. The results of the present study, in conjunction with those of our previous animal studies, suggest that PET with ^{11}C-DAG in post-MI patients can be used to visualize the myocardial phosphoinositide cycle that is activated in the process of LV remodeling, providing a useful tool for noninvasive assessment of the downstream signaling pathway of neurohumoral factors such as angiotensin II, endothelin-1, and norepinephrine.

The results of our present study are in agreement with several earlier reports demonstrating that the phosphoinositide cycle as well as its upstream and downstream pathways may contribute greatly to the development of cardiac hypertrophy and failure in animal models. Ju et al. demonstrated that the myocardial $G_{q\alpha}$ protein and phospholipase $C_{\beta1}$ pathways, located upstream of the phosphoinositide cycle, was upregulated in a rat model of MI (*19*). Kawaguchi et al. reported that myocardial accumulation of inositol 1,4,5-trisphosphate and diacylglycerol, both of which are second messengers of the phosphoinositide cycle, significantly increased in isolated cardiac myocytes from spontaneously hypertensive rats (*20*). It was unknown, however, whether the phosphoinositide cycle plays a crucial role in humans in the development of post-MI LV remodeling, cardiac hypertrophy, and heart failure because no strategy for in vivo assessment of the myocardial phosphoinositide cycle was available. In this regard, we believe that PET with ^{11}C-DAG provides a new tool to assess the myocardial phosphoinositide cycle in humans in vivo.

Discrepancy Between Animal and Human Studies

In our previous studies (*12*) using quantitative autoradiography in rats 3 wk after MI, intravenously administered ^{11}C-DAG accumulated in both infarcted and noninfarcted myocardium. The ^{11}C-DAG accumulation in the infarcted myocardium, however, was not visualized in the present study. In our previous animal experiment, the accelerated ^{11}C-DAG accumulation in the infarcted myocardium 3 wk after the onset of MI was associated with abundant inflammatory cells, such as macrophages and myofibroblasts. Fur-

thermore, ^{11}C-DAG uptake in the infarcted myocardium in rats significantly decreased 10 wk after MI, and this decrease was associated with the decreased number of inflammatory cells (*13*). Since we investigated the post-MI patients 20 ± 16 mo after the onset of MI in the present study, the healing process in the infarcted myocardium may have been almost completed, and there may have been few inflammatory cells in the scar tissue. The difference in the time points between the previous animal experiments and the present clinical study, therefore, may explain the difference in the ^{11}C-DAG uptake in the infarcted myocardium. Furthermore, the limited spatial resolution of PET compared with that of autoradiography may have attenuated the recovery of ^{11}C-DAG counts in the infarcted myocardium because of the decreased thickness of the scar tissue compared with the viable remote myocardium. Therefore, the difference in the spatial resolution of the modality may have contributed partially at least to the difference in ^{11}C-DAG accumulation in the infarcted myocardium between the previous animal studies and the present clinical study.

Myocardial ^{11}C-DAG Accumulation in Noninfarcted Heart

In the present study, mild accumulation of ^{11}C-DAG was observed in myocardium of the healthy volunteers. An in vitro experimental study by Steinberg and Alter demonstrated that cardiac myocytes accumulate inositol phosphates even at the baseline condition (*21*). Although the crucial roles of the myocardial phosphoinositide cycle in pathologic conditions have been established (*22–24*), it is unclear how the phosphoinositide cycle participates in the maintenance of homeostasis in the cardiovascular system. Further study is needed to clarify the implications of the mild ^{11}C-DAG accumulation in the myocardium of the healthy volunteers.

Myocardial ^{11}C-DAG Accumulation and Medication

Although most post-MI patients in the present study had been treated with angiotensin-converting enzyme inhibitors or angiotensin receptor blockers, the myocardial accumulation of ^{11}C-DAG in some patients was still high. There are 2 possible explanations regarding this issue. First, as shown

in Table 1, the dose of medication to suppress the renin–angiotensin system might not have been sufficiently high, and no patients received both angiotensin-converting enzyme inhibitors and angiotensin receptor blockers. The medication in some post-MI patients might not have been sufficient to reduce the myocardial accumulation of ^{11}C-DAG since an additional analysis showed that the myocardium-to-LA chamber ratio of ^{11}C-DAG was not significantly different between the post-MI patients treated with and without angiotensin-converting enzyme inhibitors or angiotensin II receptor blockers (1.80 ± 0.36 vs. 1.48 ± 0.08, respectively; $P = 0.16$). Therefore, it would be very interesting to assess the myocardial ^{11}C-DAG accumulation after increasing the dose of angiotensin-converting enzyme inhibitors or angiotensin receptor blockers or after adding either of these drugs in patients for whom they were not initially prescribed. Second, the myocardial phosphoinositide cycle has been shown to mediate signaling not only from angiotensin II but also from endothelin-1 and α_1-adrenergic receptor agonists (6). The effects of blockades for endothelin-1 and α_1-adrenergic agonists should also be investigated.

Limitations

Some limitations of this study should be mentioned:

- Because we did not correct for the partial-volume effect on myocardial ^{11}C-DAG counts, it is possible that the high myocardial ^{11}C-DAG accumulation shown in some post-MI patients was due to the increased wall thickness. This would be unlikely, however, because the myocardium-to-LA chamber ratio of ^{11}C-DAG did not correlate with the ventricular wall thickness as described earlier. Furthermore, the wall thickness of the post-MI patients was not significantly increased compared with that of the healthy volunteers, as also demonstrated earlier. Therefore, the partial-volume effect would not likely explain the increased myocardium-to-LA chamber ratio of ^{11}C-DAG accumulation in the post-MI patients.

- The variation in the period after the onset of MI in our patients might have had an impact on the LV remodeling, as would the difference in the initial extent of myocardial infarction. However, the period after the onset of MI was not significantly correlated with the myocardium-to-LA chamber ratio of ^{11}C-DAG in the present study ($r = 0.48$, $P = 0.10$). Therefore, the myocardial accumulation of ^{11}C-DAG could not be simply explained by the variation in the time after MI in our patient group.

- In the present study, we could not assess the metabolic fate of ^{11}C-DAG that accumulated in the myocardium of the study patients because myocardial biopsy was not performed after the injection of ^{11}C-DAG. In our previous animal study (12), although the intermediates of the phosphoinositide cycle were a predominant metabolic fate of ^{11}C-DAG, we also found ^{11}C radioactivity in butyryl CoA, phosphatidylcholine, and phosphatidylethanolamine, which are not intermediates of the phosphoinositide cycle. Further studies, including myocardial biopsy after the ^{11}C-DAG injection, is required to determine the metabolic fate of ^{11}C-DAG that accumulates in the human myocardium.

CONCLUSION

Although we need further studies with a larger population to establish the clinical significance of PET with ^{11}C-DAG in post-MI patients, the results of the present study suggest that myocardial accumulation of ^{11}C-DAG assessed by PET in post-MI patients is related to LV enlargement, LV systolic dysfunction, and the plasma BNP level. This new imaging strategy based on intracellular signaling may contribute to optimizing the choice of therapies to prevent LV remodeling and subsequent heart failure in post-MI patients.

ACKNOWLEDGMENTS

REFERENCES

1. Pfeffer MA, Braunwald E. Ventricular remodeling after myocardial infarction: experimental observation and clinical implications. *Circulation.* 1990;81:1161–1172.

2. Pfeffer JM, Pfeffer MA, Braunwald E. Influence of chronic captopril therapy on the infarcted left ventricle of the rat. *Circ Res.* 1985;57:84–95.

3. Pfeffer MA, Braunwald E, Moye LA, et al. Effect of captopril on mortality and morbidity in patients with left ventricular dysfunction after myocardial infarction: results of the survival and ventricular enlargement trial—The SAVE Investigators. *N Engl J Med.* 1992;327:669–677.

4. The Acute Infarction Ramipril Efficacy (AIRE) study investigators. Effect of ramipril on mortality and morbidity of survivors of acute myocardial infarction with clinical evidence of heart failure. *Lancet.* 1993;342:821–828.

5. Brown NJ, Vaughan DE. Angiotensin-converting enzyme inhibitors. *Circulation.* 1998;97:1411–1420.

6. De Jonge HW, Van Heugten HA, Lamers JM. Signal transduction by the phosphatidylinositol cycle in myocardium. *J Mol Cell Cardiol.* 1995;27:93–106.

7. Allo SN, Carl LL, Morgan HE. Acceleration of growth of cultured cardiomyocytes and translocation of protein kinase C. *Am J Physiol.* 1992;263:C319–C325.

8. Sadoshima J, Izumo S. Mechanical stretch rapidly activates multiple signal transduction pathways in cardiac myocytes: potential involvement of an autocrine/paracrine mechanism. *EMBO J.* 1993;12:1681–1692.

9. Bowling N, Walsh RA, Song G, et al. Increased protein kinase C activity and expression of Ca^{2+}-sensitive isoforms in the failing human heart. *Circulation.* 1999;99:384–391.

10. Braun MU, LaRosee P, Schon S, et al. Differential regulation of cardiac protein kinase C isozyme expression after aortic banding in rat. *Cardiovasc Res.* 2002;56:52–63.

11. Imahori Y, Fujii R, Ueda S, et al. Membrane trapping of carbon-11-labeled 1,2-diacylglycerols as a basic concept for assessing phosphatidylinositol turnover in neurotransmission process. *J Nucl Med.* 1992;33:413–422.

12. Chida M, Kagaya Y, Imahori Y, et al. Visualization of myocardial phosphoinositide turnover with 1-[1-^{11}C]-butyryl-2-palmitoyl-rac-glycerol in rats with myocardial infarction. *J Nucl Med.* 2000;41:2063–2068.

13. Kagaya Y, Chida M, Imahori Y, et al. Effect of angiotensin converting enzyme

inhibition on myocardial phosphoinositide metabolism visualized with 1-[1-^{11}C]-butyryl-2-palmitoyl-rac-glycerol in myocardial infarction in the rat. *Eur J Nucl Med.* 2002;29:1516–1522.

14. Schiller NB, Shah PM, Crawford M, et al. Recommendations for quantitation of the left ventricle by two-dimensional echocardiography. *J Am Soc Echocardiogr.* 1989;2:358–367.

15. Dodge HT, Sandler H, Ballew DW, et al. The use of biplane angiocardiography for the measurement of left ventricular volume in man. *Am Heart J.* 1960;60: 762–776.

16. Imahori Y, Fujii R, Ueda S, et al. Phosphoinositide turnover imaging linked to muscarinic cholinergic receptor in the central nervous system by positron emission tomography. *J Nucl Med.* 1993;34:1543–1551.

17. Imahori Y, Ohmori Y, Fujii R, et al. Rapid incorporation of carbon-11-labeled diacylglycerol as a probe of signal transduction in glioma. *Cancer Res.* 1995;55: 4225–4229.

18. Matsumoto K, Imahori Y, Fujii R, et al. Evaluation of phosphoinositide turnover on ischemic human brain with 1-[1-^{11}C]-butyryl-2-palmitoyl-rac-glycerol using PET. *J Nucl Med.* 1999;40:1590–1594.

19. Ju H, Zhao S, Tappia PS, et al. Expression of Gq alpha and PLC-beta in scar and border tissue in heart failure due to myocardial infarction. *Circulation.* 1998;97: 892–899.

20. Kawaguchi H, Sano H, Iizuka K, et al. Phosphatidylinositol metabolism in hypertrophic rat heart. *Circ Res.* 1993;72:966–972.

21. Steinberg SF, Alter A. Enhanced receptor-dependent inositol phosphate accumulation in hypoxic myocytes. *Am J Physiol.* 1993;265:H691–H699.

22. Nishizuka Y. Intracellular signaling by hydrolysis of phospholipids and activation of protein kinase C. *Science.* 1992;258:607–614.

23. Pfeffer MA. Left ventricular remodeling after acute myocardial infarction. *Annu Rev Med.* 1995;46:455–466.

24. LaMorte VJ, Thorburn J, Absher D, et al. Gq- and ras-dependent pathways mediate hypertrophy of neonatal rat ventricular myocytes following alpha 1-adrenergic stimulation. *J Biol Chem.* 1994;269:13490–13496.

The Journal of
NUCLEAR MEDICINE

Myocardial ^{11}C-Diacylglycerol Accumulation and Left Ventricular Remodeling in Patients After Myocardial Infarction

Hiroki Otani, Yutaka Kagaya, Yoshio Imahori, Satoshi Yasuda, Ryo Fujii, Masanobu Chida, Shigeto Namiuchi, Morihiko Takeda, Masahito Sakuma, Jun Watanabe, Tatsuo Ido, Hiroshi Nonogi and Kunio Shirato

This article and updated information are available at:
http://jnm.snmjournals.org/content/46/4/553

Information about reproducing figures, tables, or other portions of this article can be found online at:
http://jnm.snmjournals.org/site/misc/permission.xhtml

Information about subscriptions to JNM can be found at:
http://jnm.snmjournals.org/site/subscriptions/online.xhtml

SNMMI
SOCIETY OF
NUCLEAR MEDICINE
AND MOLECULAR IMAGING